



UvA-DARE (Digital Academic Repository)

Formation and evolution of hybrid He-CO white dwarfs and their properties

Zenati, Y.; Toonen, S.; Perets, H.B.

DOI

[10.1093/mnras/sty2723](https://doi.org/10.1093/mnras/sty2723)

Publication date

2019

Document Version

Final published version

Published in

Monthly Notices of the Royal Astronomical Society

[Link to publication](#)

Citation for published version (APA):

Zenati, Y., Toonen, S., & Perets, H. B. (2019). Formation and evolution of hybrid He-CO white dwarfs and their properties. *Monthly Notices of the Royal Astronomical Society*, 482(1), 1135-1142. <https://doi.org/10.1093/mnras/sty2723>

General rights

It is not permitted to download or to forward/distribute the text or part of it without the consent of the author(s) and/or copyright holder(s), other than for strictly personal, individual use, unless the work is under an open content license (like Creative Commons).

Disclaimer/Complaints regulations

If you believe that digital publication of certain material infringes any of your rights or (privacy) interests, please let the Library know, stating your reasons. In case of a legitimate complaint, the Library will make the material inaccessible and/or remove it from the website. Please Ask the Library: <https://uba.uva.nl/en/contact>, or a letter to: Library of the University of Amsterdam, Secretariat, P.O. Box 19185, 1000 GD Amsterdam, The Netherlands. You will be contacted as soon as possible.

Formation and evolution of hybrid He–CO white dwarfs and their properties

Yossef Zenati,¹★ Silvia Toonen^{1,2} and Hagai B. Perets¹ 

¹Physics Department, Technion – Israel Institute of Technology, Haifa 3200004, Israel

²Anton Pannekoek Institute for Astronomy, University of Amsterdam, NL-1090 GE Amsterdam, the Netherlands

Accepted 2018 October 4. Received 2018 October 4; in original form 2018 March 11

ABSTRACT

White dwarfs (WDs) are the stellar core remnants of low mass ($\lesssim 8 M_{\odot}$) stars. They are typically divided into three main composition groups: oxygen–neon (ONe), carbon–oxygen (CO), and helium (He) WDs. The evolution of binary systems can significantly change the evolution of the binary stellar components. In particular, stripping the envelope of an evolved star can give rise to a core remnant, which can later evolve into a WD with significantly different composition. Here we focus on the formation and evolution of hybrid HeCO WDs. We follow the formation and stellar evolution of such WDs for a range of initial conditions and provide their detailed structure, mass–radius relation and luminosity–temperature evolution. We confirm that both low-mass WDs ($< 0.45 M_{\odot}$, typically thought to be He-WDs) and intermediate-mass WDs ($0.45 < M_{\text{WD}} \leq 0.7$, typically thought to be CO-WDs) could in fact be hybrid HeCO WDs, with 5–25 (75–95) per cent of their mass in He (CO). We use population synthesis calculations to infer the birth rate and properties of such WDs. We find that hybrid HeCO-WD comprise the majority of young (< 2 Gyr) WDs in binaries, but are rarer among older WDs in binaries. The high frequency and large He content of such WDs could have an important role in WD–WD mergers, and may give rise to sub-Chandrasekhar thermonuclear supernova explosions.

Key words: stars: evolution – stars: horizontal branch – stars: mass-loss – white dwarfs.

1 INTRODUCTION

White dwarfs (WDs) are the stellar core remnants of low-mass ($\lesssim 8 M_{\odot}$) stars that formed following their post-main-sequence (MS) evolution. They are composed mostly of electron-degenerate matter, and are divided into several types, including WDs composed of carbon–oxygen (CO) and oxygen–neon (ONe) WDs, corresponding to the stellar evolutionary end points of intermediate and high-mass stars, respectively. The minimum mass of a present-day WD formed through stellar evolution of a single star is in the range ~ 0.50 – $0.52 M_{\odot}$ arising from the lowest mass stars with lifetimes shorter than the age of the universe (1.01 down to $0.84 M_{\odot}$ for $Z = 1.5 Z_{\odot}$ down to $Z = 0.1 Z_{\odot}$, respectively, calculated using the SeBa binary population synthesis module (Toonen, Nelemans & Portegies Zwart 2012) prescriptions based on the stellar evolutionary tracks by Hurley, Pols & Tout (2000). Such WDs would be CO WDs. However, binary evolution can change these outcomes and produce different types of WDs and allowing for a

much lower mass range (e.g. Kippenhahn & Weigert 1990; Marsh, Dhillon & Duck 1995; Han et al. 2002; Rebassa-Mansergas et al. 2011, and references therein), as first observed by Marsh et al. (1995).

In interacting binaries each of the stellar component may fill its Roche lobe (Roch lobe overflow; RLOF), and may also evolve into a common envelope (Ivanova et al. 2013) configuration, and be stripped of part of its hydrogen/helium-rich envelope during its evolution on the main sequence (MS) or later on the red giant branch (RGB; or the asymptotic giant branch, AGB) stage. The altered evolution of evolved stars can give rise to qualitatively different evolution and the formation of present-day very low-mass (VLM; $< 0.45 M_{\odot}$; e.g. Iben & Tutukov 1985) WDs. The evolution and final outcomes of the binary evolution strongly depend on the initial conditions: the mass of the stellar components and their initial separation. In particular, WDs of masses lower than $0.45 M_{\odot}$ are typically thought to be Helium (He)-WDs formed through this channel (e.g. Iben & Tutukov 1985; Nelemans et al. 2001b; Han et al. 2002; Istrate et al. 2016; Zhang et al. 2018). However, the complex binary evolution channel can give rise to VLM (as well as more massive) *hybrid-WDs*, composed of significant

* E-mail: oyossefzm@gmail.com

fractions of both CO and He. Such white dwarfs descend from stars which fill their Roche lobes in the stage of hydrogen burning in a shell, become hot sub-dwarfs in the He-burning stage, but do not experience envelope expansion after the formation of a degenerate carbon–oxygen core (Iben & Tutukov 1985). Note that hybrid CO–ONe WDs were also suggested to exist (Denissenkov et al. 2013); these are not related to this study where we only discuss HeCO WDs.

The exact definition of a hybrid HeCO WD is somewhat arbitrary; one can consider a hybrid HeCO WD as any WD in which no less than some fraction f_{He} of the mass is composed of He, and no less of a fraction f_{CO} of the mass is composed of CO. In practice, in all of the hybrid WDs we find the mass is dominated by CO. Here we focus on such hybrid WDs; we explore their properties and evolutionary channels, and discuss their implications on our understanding of WDs and their structure, which are strongly dependent on the composition. Not less important, HeCO WDs may have an important role in affecting the outcomes of WD–mergers, and in particular the possible production of thermonuclear SNe from double-degenerate WD mergers. For the latter, the existence of a significant mass in He can catalyze thermonuclear SN explosions even in sub-Chandrasekhar mass WDs (e.g. Woosley, Taam & Weaver 1986; Iben et al. 1987; Livne & Glasner 1990; Bildsten et al. 2007; Waldman et al. 2011). Hence, understanding of hybrid WDs is critical for a wide range of compact objects as well as their potential explosive mergers.

HeCO WDs have been first discussed by Iben & Tutukov (1985) who suggested that a significant fraction of the VLM WDs could be HeCO WDs rather than He (only) WDs. The possibility of HeCO WDs, later termed hybrid WDs, have been then further discussed (though briefly) in various contexts (Tutukov & Yungelson 1992; Iben et al. 1997). Studies of stellar cores have already shown early on (Iben 1967) that there exists a lower limit for the core mass of about $\sim 0.3 M_{\odot}$ below which cooling of degenerate matter prevents He-ignition. Consequently, one should expect a similar lower limit for the mass of CO–WD cores. Later studies of VLMs by Althaus et al. (2004) and Panei et al. (2007) further confirmed this, showing that binary evolution of low mass ($< 3.16 M_{\odot}$) progenitor stars can give rise to WDs in the mass range $0.35\text{--}0.45 M_{\odot}$ mostly composed of oxygen. Follow-up studies by Prada Moroni & Straniero (2009) had been able to produce a CO WD of $0.33 M_{\odot}$ consistent with the lower limit expected for such WDs. More recent studies have further developed the study of VLM He WDs (and references therein, Istrate et al. 2016; Zhang et al. 2018). All of these later studies explored the possibility of VLM He WDs, with little discussion of the potential of hybrid He–CO VLMs. Our focus is exploring the range of possible hybrid HeCO WDs and their properties, map the possible range of He to CO mass fractions in these WDs and characterize their structure and mass–radius relationship. Our detailed stellar evolution findings (using the MESA code; Paxton et al. 2011, 2015) can be used to direct the more simplified population synthesis models in order to characterize the general properties of hybrid-WD that form, their binary system progenitors and the type of double-degenerate mergers in which they participate. The outcomes of the latter are further explored in forthcoming publications.

The paper is structured as follows. First (Section 2), we describe the methods used to explore the detailed stellar evolution models (using the MESA code) and population studies (using the SeBa population synthesis code; Section 3) for the formation of hybrid-WDs. We present our main results in Section 4 and then discuss the implications of hybrid-WDs, and summarize (Section 5).

2 DETAILED STELLAR EVOLUTION: METHODS

The evolution of a stripped star in an interacting binary and its He core is significantly altered compared with the uninterrupted evolution of a non-interacting (single) star. When most of the red giant envelope is removed, hydrogen shell burning is quelled, the He-core keeps growing, and the star begins to contract. If the He core is sufficiently massive, the contraction will eventually trigger He ignition (see Iben & Tutukov 1985) and the formation of a CO core; the He to CO ratio will then be determined by the specific detailed evolution of He burning into CO, and mass-loss through winds from the envelope.

In order to follow the complex evolution, we begin by considering a range of initial binary conditions. The initial binary separations are chosen such that the lower mass binary component will eventually fill its Roche lobe. The stellar evolutionary tracks of binary components are followed from the pre-MS stage until the final production of the WD. We mapped these conditions into the stellar evolution code MESA and the used the binary mode (Paxton et al. 2015) to follow their evolution for the range of initial conditions. The MESA binary-mode follows the evolution of both stars and their orbits, and prescribe the mass-loss according to binary separation. A different approach is to not account for the evolution of the binary and instead just introduce an artificial mass-loss from a single star, without accounting for the binary evolution in detail. In this single-mode case we introduce an effective mass-loss from a single star on the RGB without accounting for the evolution of a binary companion and its orbit. Mass-loss was introduced in these single-star cases when the conditions for the radius and core mass are such that RLOF is expected.

Common envelope stripping is thought to occur on very short time-scales, hence leading to very large mass-loss rates. Exact studies of these can be done using hydrodynamical codes. However, here we are interested in the long-term evolution following the mass-loss. As long as the mass-loss time-scales are significantly shorter than the evolutionary time, the exact mass-loss prescription is not important. Since the mass-loss in common-envelope stripping cannot be accurately modelled in a stellar evolution code, we effectively mimic the stripping through the use of the mass-loss module used in the code, i.e. wind mass-loss. We used the highest mass-loss rates for which we could get numerical convergence, typically $\dot{M} \sim 10^{-4} M_{\odot} \text{ yr}^{-1}$, though lower mass-loss rates of $\dot{M} \sim 10^{-5} M_{\odot} \text{ yr}^{-1}$ produce the same results. In the first two models (1,2) we used $\dot{M} \sim 10^{-5} M_{\odot} \text{ yr}^{-1}$. In practice, the mass-loss rate issue is not fine-tuned, and the appropriate conditions can be fulfilled over a range of stellar radii (as indicated in Table 1) once the star experiences the first thermal pulse, or in some cases the second or third thermal pulses. Generally, the binary module is potentially more accurate, but it gives rise to more complexities and numerical difficulties. Therefore we used both approaches, showing, as expected, very similar evolution of the stripped star, and hence also showing that indeed the exact mass-loss prescription is not important. In the parameter range studied the final outcomes of the evolution produce qualitatively and quantitatively similar results throughout our simulations, we therefore show the results only for the choice of the middle point in the relevant range.

In all cases where both the binary and single mode models converged we obtained consistent final outcomes, further validating both these approaches. In some cases, however, only our altered single mode model numerically converged, in which case we report the results only from the single-mode model. The prop-

Table 1. Characteristics of a binary succeed to survive until the hybrid WD phase. The M_1 is the donor mass, q is the mass ratio, P is the initial period for the binary in RLOF. $\log T_{\text{eff}}$ is the effective temperature when the donor gets our condition. M_{WD}^f is the final mass of the donor (hybrid WD mass), $M_{\text{He4}}^f, M_{\text{C12}}^f, M_{\text{O16}}^f$ is the final amount of He4, C12, O16.

#	$M_1 [M_{\odot}]$	q	P [d]	$\log T_{\text{eff}}$	$M_{\text{WD}}^f [M_{\odot}]$	$M_{\text{He4}} [M_{\odot}]$	$M_{\text{C12}} [M_{\odot}]$	$M_{\text{O16}} [M_{\odot}]$	$M_{\text{HI}} [M_{\odot}]$	Modelling ^a
1	2.50	0.81	5.01	5.0	0.36	(19%), (0.07)	(42%), (0.15)	(39%), (0.14)	5.4×10^{-4}	S,B
2	2.66	0.78	4.5	5.0	0.41	(25%), (0.1)	(38%), (0.16)	(37%), (0.15)	5.0×10^{-4}	B
3	2.75	0.79	5.00	5.0	0.44	(25%), (0.11)	(37%), (0.16)	(38%), (0.17)	6×10^{-4}	S
4	2.85	0.36	7.5	5.2	0.46	(21%), (0.10)	(38%), (0.17)	(41%), (0.19)	3×10^{-4}	B
5	3.01	0.74	6.28	5.0	0.53	(14%), (0.074)	(43%), (0.23)	(43%), (0.23)	2×10^{-5}	S,B
6	3.20	0.71	6.28	5.2	0.58	(9%), (0.052)	(45%), (0.26)	(46%), (0.26)	4.1×10^{-5}	S,B
7	3.41	0.70	7.00	5.2	0.63	(5%), (0.03)	(48%), (0.3)	(47%), (0.29)	3.0×10^{-4}	S
8	3.50	0.77	7.44	5.2	0.66	(4%), (0.026)	(48%), (0.31)	(48%), (0.31)	3.2×10^{-4}	S,B
9	3.72	0.66	8.50	5.2	0.68	(2%), (0.015)	(49%), (0.33)	(49%), (0.33)	1.6×10^{-4}	S,B
10	4.00	0.78	11.13	5.2	0.74	(<1.5%), (<0.01)	(49%), (0.36)	(49%), (0.36)	7.3×10^{-4}	S,B

^aType of modelling using the binary (B) evolution mode in MESA or an effective binary evolution using a single (S) star module.

erties of the initial binaries extend over a range of initial primary component mass ($2.5 M_{\odot} \leq M_{\text{donor}} \leq 4 M_{\odot}$) and mass ratios ($0.65 \lesssim q = M_{\text{donor}}/M_{\text{companion}} \lesssim 0.81$; with the exception of one case with $q = 0.36$); the detailed models and their outcomes are summarized in Table 1. We also modelled donor stars with lower masses ($< 2 M_{\odot}$), but these only produced He WDs, or He WDs with a very low fraction of CO, and we therefore do not consider these as hybrid HeCO WDs.

Though some models had been difficult to converge numerically, we were able to resolve the evolution of these binaries through the whole relevant mass range and mass ratio. In all these cases we were able to produce a hybrid HeCO WD. In the following we discuss in detail our assumptions and initial conditions. All of our models (and MESA inlist files) are openly available at GitHub as to enable simple reproduction of the results (github.com/Hybrid-WD).

In the following we list our detailed assumptions and considerations:

(i) Metallicity: all models are of Solar metallicity stars $Z = Z_{\odot} = 0.02$.

(ii) Mass transfer: we use a range of 10^{-8} – $10^{-10} M_{\odot} \text{ yr}^{-1}$ for the *min mdot for implicit* parameter.

(iii) Mixing: we set $\alpha = l/H_p = 1.5$ as the ratio of typical mixing length to the local pressure scale height, where l is the mixing length, α is a free parameter, and H_p is the pressure scale height. The parameters for the semiconvective mixing and thermohaline mixing are taken to be 0.01 and 2, respectively (Farmer et al. 2016).

(iv) Nuclear reaction network: we use a 75 isotope nuclear reaction network. It contains the relevant isotopes needed for He, carbon, and oxygen burning.

(v) Stopping condition: we stop the evolution once the star becomes fully degenerate WD and no further evolution, beside WD cooling is observed. Our condition effectively translates to WD luminosity and temperature that fall below $L \leq 1.8 L_{\odot}$; $T_{\text{eff}} \leq 5.1 T_{\odot, \text{eff}}$ (or in some cases, $L \leq 1.12 L_{\odot}$; $T_{\text{eff}} \leq 4.94 T_{\odot, \text{eff}}$), respectively.

(vi) Mass-loss: the effective mass-loss is due to common-envelope ejection, which cannot be modelled in the stellar evolution models, instead we use a fast wind mass-loss prescription at to mimic the effective mass-loss in the binary interaction. The effective mass-loss used is $\dot{M} = 10^{-4} M_{\odot} \text{ yr}^{-1}$ for all single-mode models beside models 1 and 2 (see table) for which we used $\dot{M} = 10^{-5} M_{\odot} \text{ yr}^{-1}$. In order to ensure that the mass of the star is appropriately adjusted following the mass-loss, we let the star relax afterwards.

(vii) Overshoot: the optimal overshoot parameter enabling numerical convergence for the whole mass range (for 2.5 – $4 M_{\odot}$) was found to be $f_{\text{ov}} = 0.0016$.

(viii) We note that the use of the MESA code for modelling processes occurring on dynamical time-scales, and for which 3D aspects might be important may miss key features of this rapid phase that could have significant effects on the further evolution of the stars. Future codes may better resolve this general issue (Mocák et al. 2010).

3 POPULATION SYNTHESIS MODELS

The formation and evolution of interacting binaries producing hybrid-WDs are simulated with the binary population synthesis (BPS) code SEBA (Portegies Zwart & Verbunt 1996; Toonen et al. 2012; Toonen & Nelemans 2013). SEBA is a *fast* code for simulating binary evolution based on parametrized stellar evolution, including processes such as mass transfer episodes, common-envelope evolution, and stellar winds. We employ SeBa to generate a large population of binaries on the zero-age MS, we simulate their subsequent evolution, and extract those that produce hybrid – HeCO WDs.

It was shown in Toonen et al. (2014) that the main sources of differences between different BPS codes are due to the choice of input physics and initial conditions. Here we focus only on a specific set of choices, and use the detailed stellar evolution models to test the BPS models predictions for hybrid WDs. A wider range of initial conditions and physical assumptions will be explored in future work, where hybrid WDs may play a role in the evolution of double degenerate (WD–WD, NS–WD, and BH–WD) mergers.

The basic conditions and assumptions we use embody a classical set-up for BPS calculations, and the binaries are generated and evolved in the following ways:

(i) The primary masses are drawn from a Kroupa IMF (Kroupa, Tout & Gilmore 1993) with masses in the range between 0.1 and $100 M_{\odot}$.

(ii) The secondary masses are drawn from a uniform mass ratio distribution with $0 < q \equiv M_2/M_1 < 1$ (Raghavan et al. 2010; Duchêne & Kraus 2013; De Rosa et al. 2014).

(iii) The orbital separations a follow a uniform distribution in $\log(a)$ (Abt 1983).

(iv) The initial eccentricities e follow a thermal distribution (Heggie 1975).

(v) A binary fraction \mathcal{B} of 50 per cent which is appropriate for A-type primaries (Raghavan et al. 2010; Duchêne & Kraus 2013).

(vi) Hybrid definition: unless stated otherwise, in the BPS calculations a hybrid is defined as a WD with at least 5 per cent of its mass composed of He (see Equation 1).

(vii) We allow bare degenerate helium cores to ignite if the core gets exposed (through binary interactions) when its mass is within $0.02 M_{\odot}$ of the mass where the helium flash happens (Han et al. 2002; Nelemans 2010).

(viii) We construct two BPS models that differ with respect to the common-envelope phase. This is a short phase in the evolution of a binary system when both stars share a common-envelope. Despite its strong effect on the binary orbit, common-envelope evolution is poorly understood (see e.g. Ivanova et al. 2013; for a review). We replicate model $\alpha\alpha$ and model $\gamma\alpha$ from Toonen et al. (2017). The prior is based on the classical energy balance during the common-envelope phase (Paczynski 1976; Tutukov & Yungelson 1979; Webbink 1984; Livio & Soker 1988) in which orbital energy is used with an efficiency α to unbind the envelope material of binding energy $E_{\text{gr}} = GMM_{\text{env}}/\lambda R$, with M the mass of the donor star, M_{env} its envelope mass, λ the envelope structure parameter, and R the radius of the donor star. From reconstructing the formation of the second WD for a sample of observed double WDs, Nelemans et al. (2000) derived $\alpha\lambda = 2$, which we adopt here. The latter model (model $\gamma\alpha$) is a combination of the classical α -CE based on the energy balance, and the γ -CE which is based on a balance of orbital angular momentum J as $(J_{\text{final}} - J_{\text{initial}}/J_{\text{initial}}) = \gamma \Delta M/M + m$, with m the mass of the companion, and γ the efficiency factor (Nelemans et al. 2000). In model $\gamma\alpha$ when a CE develops, the γ -formalism is applied unless the binary contains a compact object or the CE is triggered by the Darwin–Riemann instability (Darwin 1879) for which the α -formalism is adopted. Model $\gamma\alpha$ with $\gamma = 1.75$ is based on Nelemans et al. (2001a).

In principle, a stripped Helium core can be formed in two ways, either through the common envelope or the RLOF channels. If the He core is sufficiently massive ($M_c > 0.32 M_{\odot}$), He ignition can be triggered (see Iben & Tutukov 1985, leading to the formation of a CO core; the He to CO ratio will then be determined by the specific detailed evolution. For the intermediate mass stars in this channel, the He ignites under non-degenerate conditions). In the second evolutionary channel for lower mass stars (typically $< 2 M_{\odot}$), ignition of the He occurs under degenerate conditions. In this channel the progenitors are stripped close to the peak of first giant branch, contract, and then ignite (see Han et al. 2002; for details). However, our detailed stellar evolution models show that WDs produced through this channel are effectively He WDs which contain only a very small fraction of CO (< 1 per cent), and we therefore do not discuss them here. The procedure used to define hybrid WDs in the population synthesis was therefore to select all white dwarfs that have gone through one phase of mass transfer in which the hydrogen envelope is stripped, but did not have a second phase of mass transfer in which the helium atmosphere would have been stripped. From these we then selected those WDs that are in the mass range as determined by our stellar evolution models.

4 RESULTS

4.1 Detailed stellar evolution models

Table 1 and Figs 1–4 summarize the results for the mass, composition, and structure of hybrid WDs as a function of their final mass, resulting from our detailed stellar evolution models. Although hybrids of different masses are produced from binaries which differ in

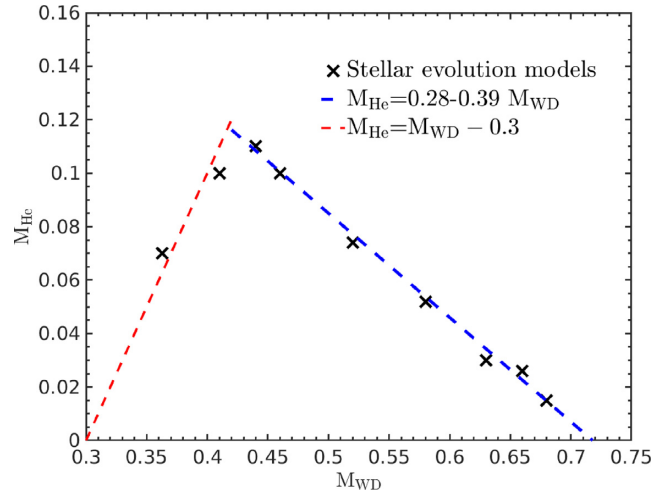


Figure 1. The He mass versus total mass of He WDs from the detailed stellar evolution models. The blue line depicts a linear fit for the range $0.4 \leq M_{\text{WD}} \leq 0.72$ and the red dashed–dotted line shows the expected dependence once the CO core–mass reaches its lower possible limit of $0.3 M_{\odot}$.

various aspects (initial mass, mass ratio, separation etc.), the final compositions form a fairly continuous sequence for most of the mass range, with He mass fractions in the range 2–25 per cent (see Fig. 1). As expected, the He forms an outer shell around the CO core, with only a very small layer of mixed CO–He composition (see Fig. 4).

Our detailed stellar evolution models suggest that the He mass in the WD M_{He} can be approximated by

$$M_{\text{He}} = 0.28 - 0.39M_{\text{WD}}, \quad (1)$$

for most of the mass range ($0.4 \leq M_{\text{WD}} \leq 0.7$, where M_{WD} is the mass of the WD). This is also approximately consistent with estimates for the core mass of He stars at which point He burning is quenched as found by Paczyński (1971) and implies there is a maximum mass for hybrids. The maximum mass of a hybrid WD is therefore $\sim 0.72 M_{\odot}$, for which the He mass goes to zero. However, for a more conservative limit, requiring a significant fraction of the WD mass to be in He (e.g. > 5 per cent), the maximum mass becomes $0.63 M_{\odot}$. As mentioned earlier, studies of stellar cores have shown early-on Iben (1967) that there exists a lower limit for the core mass of about $\sim 0.3 M_{\odot}$ below which cooling of degenerate matter prevents He-ignition. We therefore expect that the burned He, i.e. the CO core of the hybrids should not be smaller than this critical mass. This is indeed consistent with observed change in behaviour of the $M_{\text{WD}} - M_{\text{He}}$ dependence once the CO core approaches this limit – the CO core mass saturates to $0.3 M_{\odot}$ and the effective behaviour is

$$M_{\text{He}} = M_{\text{WD}} - 0.3, \quad (2)$$

4.1.1 Evolution on the HR diagram

In Fig. 2 we show the evolution of the HeCO WD progenitor on the HR diagram for one of our models. Other cases (not shown) show a qualitatively similar behaviour. As can be seen the evolution can be quite complex, and though we are mostly interested in the final WD configuration we refer the interested reader to Iben & Tutukov (1985) for a detailed discussion of the various evolutionary stages before the final formation of the hybrid WD. We also compare the

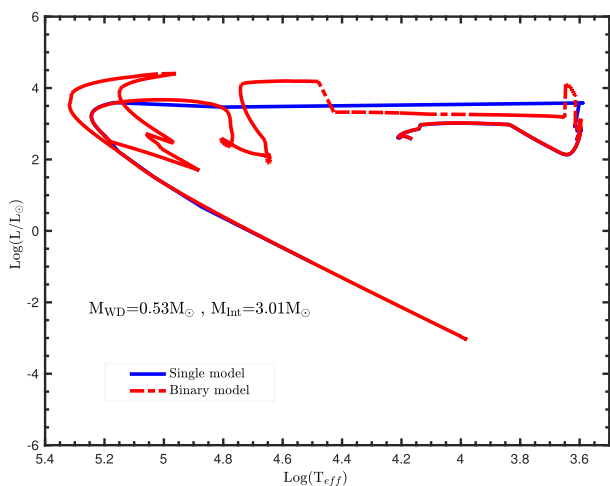


Figure 2. Comparison of the evolution using the single and binary modes. Both models begin at the same position, and mass stripping is modelled as to occur at the same evolutionary stage in both models (specifically we stripping begins once $L_{\text{nuc}}/L_{\text{ZAMS}} > 0.901$ in this case). Though the early evolution is naturally different, the two evolutionary modes converge once the effective mass-loss used effectively mimic the binary evolution. The excellent correspondence between the models supports our use of single mode models for the cases where binary evolution mode did not numerically converge.

results from the MESA binary evolution model to a more simplified single star evolution where the envelope stripping is included artificially without fully following the binary evolution. As can be seen the single models follow a different evolution at early times, but following the stripping they results in the same WD configuration and evolution, supporting their general use for modelling hybrids. This also suggests that uncertainties in the mass-transfer phase do not significantly affect the final structure of the hybrid WDs. Overall we find only small differences in the final WD configurations when we use the single and binary models, with typical C, O, and He masses differences of less than 1 per cent (besides the case of $M_{\text{WD}} = 0.58$, where a 5 per cent difference in the He abundance was found).

4.2 Structure and composition of HeCO hybrid WDs

The mass–radius relation for the progenitors of HeCO WDs as well as the HeCO WDs (once they become degenerate) is shown in Fig. 3. As expected the radii typically fall in between those of CO WDs and purely He WDs.

In Fig. 4 we present the composition structure of the hybrids. Note that a thin low-mass layer of hydrogen is typically retained in all models (see also Table 1).

4.3 Population synthesis results

We find that hybrid WDs are commonly formed. For a group of stars with a combined initial mass of $1000 M_{\odot}$, we expect 3.6–3.9 hybrids to form in a Hubble time. The birthrate of hybrids as a function of the (delay) time between the zero-age (ZAMS) main sequence and the formation of the hybrid is shown in Fig. 5 (solid black line). In the first 2 Gyrs, the birthrate is about 10^{-12} per yr per solar mass of created stars, and it then decreases to a few $\times 10^{-14} \text{ yr}^{-1} M_{\odot}^{-1}$. To put the birthrate of hybrids in perspective, we also show in Fig. 5 the birthrate distribution of white dwarfs

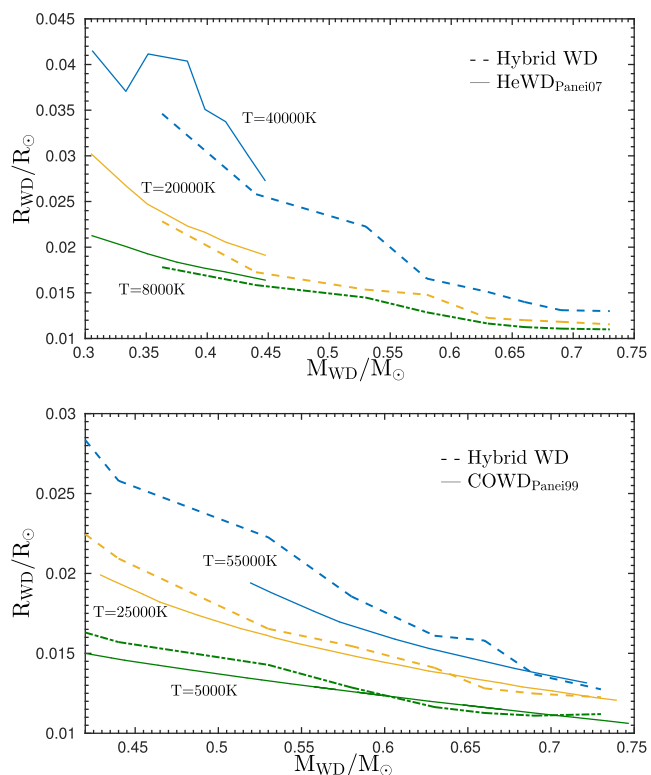


Figure 3. The mass–radius relation for hybrid HeCO WDs and their progenitors. The mass–radius relation is shown for three temperatures for each regime (comparison with He WDs on top and with CO WDs in bottom figure). As expected the radii of hybrid WDs falls in an intermediate regime between purely He WDs and purely CO WDs (e.g. compare with Panei, Althaus & Benvenuto 2000; Panei et al. 2007), besides for the most massive hybrids where the He fraction is small and the radii are comparable with that of CO WDs with a small He envelope (taken from Panei et al. 2000, 2007).

of all flavours that are formed in interacting binaries. One Gyr after star formation, roughly 50–60 per cent of newly born WDs in compact binaries are hybrids. At later times, roughly 6 per cent of the new WDs have a hybrid HeCO composition.

4.3.1 Formation channels

Most hybrids are formed from intermediate mass stars in the first channel at a time-integrated birthrate of $2.7\text{--}3.0 \times 10^{-3}$ per M_{\odot} of created stars. The masses of the hybrids span a large range, from a lower limit of $\sim 0.32 M_{\odot}$ to the upper limit set to $0.63 M_{\odot}$. The birthrate in this channel is therefore sensitive to our assumption about the minimum He fraction of a hybrid. If we are more (less) conservative with our assumption of what constitutes a hybrid WD, and include hybrids with He mass fractions only down to 10 per cent (1 per cent), the time-integrated birthrate from the first channel decreases (increases) to $2.0\text{--}2.3 \times 10^{-3}$ ($3.2\text{--}3.4 \times 10^{-3}$) per M_{\odot} of created stars. The full range of masses is reached by hybrid progenitors that fill their Roche lobe on, or before the RGB; if the progenitor loses its hydrogen envelope on the AGB, the minimum hybrid mass is $\sim 0.52 M_{\odot}$. The progenitors of the hybrids in this channel have typical ZAMS masses of 2–4 M_{\odot} , and their formation times are short, i.e. typically several hundred Myrs. This evolutionary channel therefore gives rise to low-mass WD with masses comparable to those of CO WDs typically formed only after Gyrs of evolution of single stars. The formation of hybrid is nevertheless not limited

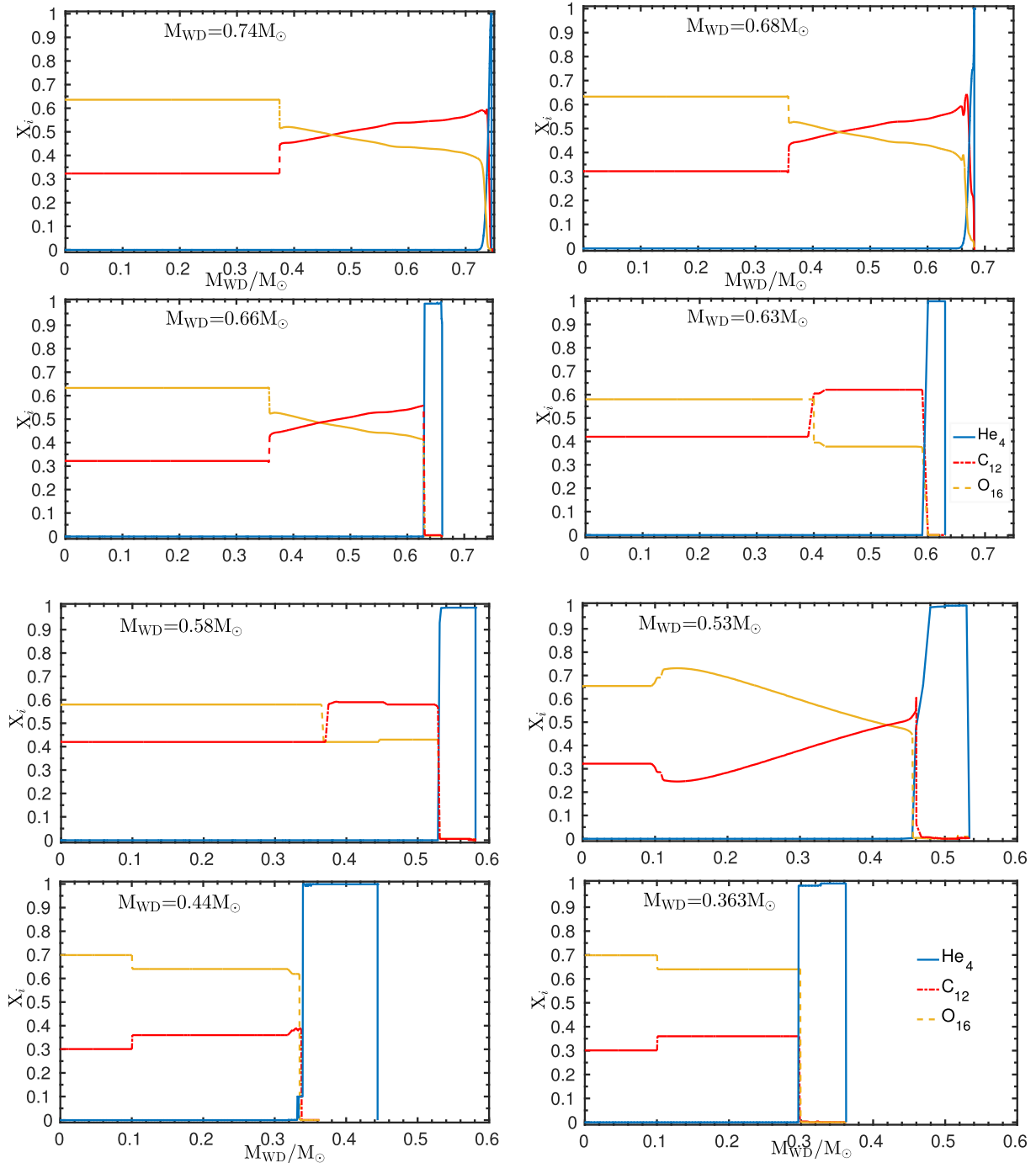


Figure 4. The composition structure of hybrid HeCO WDs for all the calculated models (see Table 1).

to this short time-scale, but can extend up to several Gyrs when it is the secondary star that becomes the hybrid instead of the primary star.

4.3.2 Evolution and mergers of hybrid-WDs

In roughly half (48–56 per cent) of the cases, the stellar components of the hybrid-WD binaries will eventually merge with one another through their late evolution. In 25–37 per cent of these mergers the hybrids merge with hydrogen-rich stellar companions, and in the other systems the hybrids merge with WD companions. Given their

large fractions among binary WDs, this suggests that a large fraction of all WD mergers involve a hybrid WD. The merger rate of hybrid white dwarfs is shown in Fig. 6 as a function of the merger time (since ZAMS). If such HeCO-CO WD mergers lead to type Ia SNe, they may potentially serve as the dominant channel for type Ia SNe, especially at early times of up to 2–3 Gyrs. These results are consistent with the results by Yungelson & Kuranov (2017), who already suggested such mergers as a dominant channel [compare our Fig. 5 with their Fig. 2, A and B channels; note that Yungelson & Kuranov (2017) consider He and HeCO WDs together, however given that the overall contribution of He WD to the mergers is

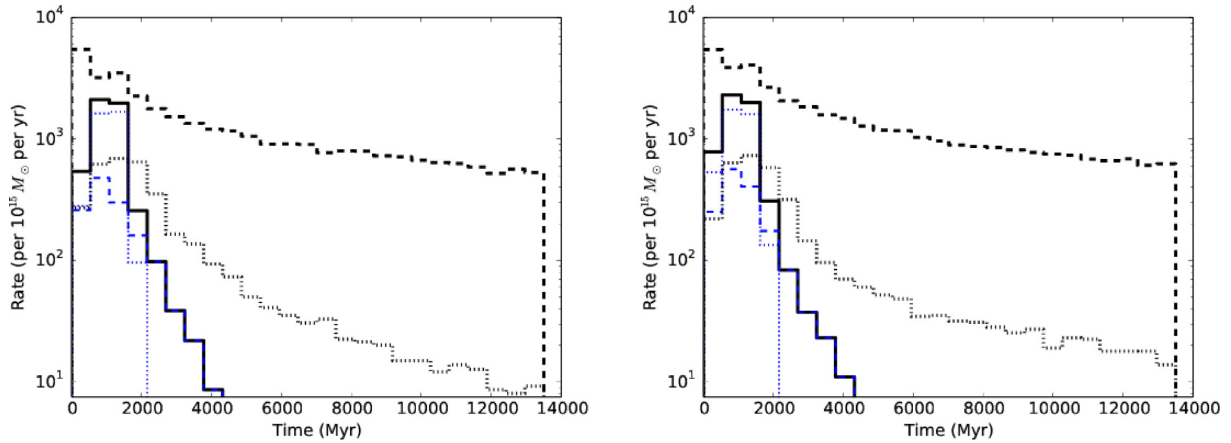


Figure 5. The formation rate of hybrid WDs assuming a single burst of star formation at time equals 0. Model $\alpha\alpha$ and model $\gamma\alpha$ for the CE-phase are shown on the left and right, respectively. Dashed (black) lines depict all type of WDs in interacting binaries, solid (black) lines depict only hybrid-WDs. Dotted (black) lines show the merger rate of systems with a hybrid (i.e. their destruction rate), dotted (thin blue) lines correspond to the main non-degenerate channel (from more massive stars); the dashed (blue) line shows the cases where the secondary is a hybrid, and the primary is a WD.

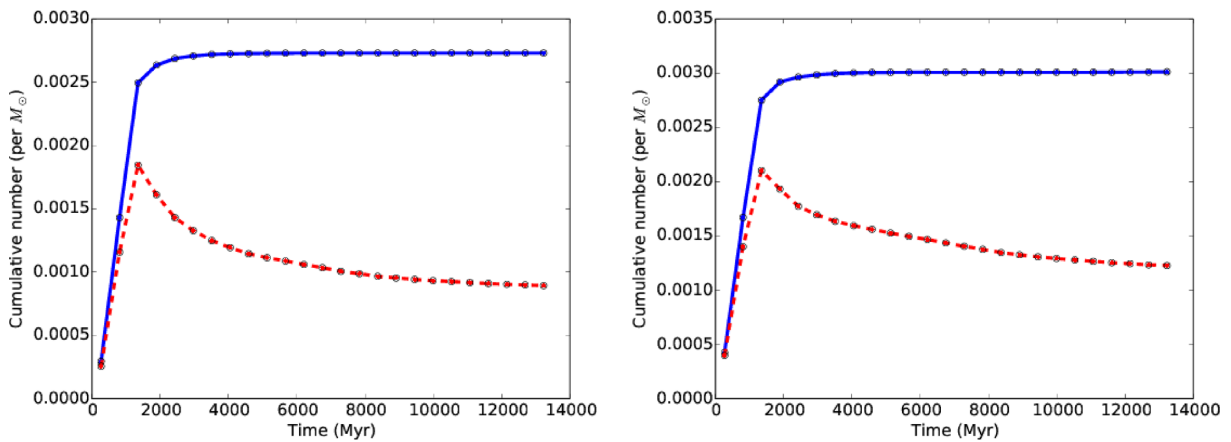


Figure 6. The total cumulative number (per solar mass) of hybrid-WD formed as a function of time since star formation (i.e. assuming a single burst of star formation at time equals 0). On the left model $\alpha\alpha$ for the CE-phase is shown, on the right model $\gamma\alpha$. Upper (blue) lines show the time integrated birth-rate of hybrid-WDs, i.e. the cumulative number of *formed* hybrid-WDs as a function of the time. Lower (red) line shows the total cumulative number of *existing* hybrids as a function of the time, i.e. after accounting for the actual lifetime – subtracting the number of hybrids destroyed (typically through mergers with their companion) from the total number of formed hybrids.

small, the figures mostly represent hybrid HeCO WDs, that can be compared with our results].

Another likely outcome is that the binary does not change significantly after the formation of the hybrid, e.g. in cases where the secondary is a low-mass MS star that does not evolve off the MS in a Hubble time. This happens for about ~ 20 – 26 per cent of the hybrids. In 14 – 31 per cent the binary experiences one or more phases of mass transfer initiated by the secondary star and forms a double white dwarf system. In about 2.0 – 3.9 per cent of systems a cataclysmic variable is formed.

5 DISCUSSION AND SUMMARY

In this work we have systematically studied the formation and evolution of hybrid HeCO WDs in binary systems. We studied a wide range of initial conditions, and explored the distribution of the hybrid-WDs properties and formation times using binary population synthesis models. Our findings suggest that hybrid HeCO WDs can form robustly, and give rise to a significant fraction of all WD binaries with 50 – 60 per cent of all young, < 2 Gyr WD

being hybrids, (but they become rare among older populations). In particular, a large fraction of all VLM WDs, especially young ones, typically considered to be He WDs could in fact be hybrids. Moreover, the mass range of hybrid WDs can extend up above to $\sim 0.62 M_{\odot}$, i.e. into the regime typically considered only for CO WDs. Therefore, observationally hybrid WDs could be misidentified as CO DB WDs, which could affect mass–radius interpretations of observations. Similarly, misidentification could also affect WD chronology estimates, given the difference in the cooling–sequences for hybrids. The hybrid WDs are composed of significant He abundance, with He mass fractions in the range 2 – 25 per cent; they reside in an intermediate mass–radius range between purely He and purely CO WDs. The latter issue, which is not included in population synthesis studies may slightly affect the later evolution and interaction of WD–WD binaries, which can strongly depend on the WD radii. We postpone further exploration of this issue for future studies. We note that the different structure and composition of hybrid WDs compared with same mass purely CO/He WDs could, in principle be probed using asteroseismology (e.g. Winget & Kepler 2008).

Given their prevalence among WD binaries, hybrid WDs may later further interact with their binary companions. In particular their role in merger of double degenerate systems (WD–WD, WD–NS, WD–BH) could be of particular interest. Such hybrids and their mergers could potentially give rise to explosive thermonuclear events with distinct properties due to the important role of the He in catalyzing more effective thermonuclear reactions and detonations (e.g. in the context of Sub-Chandrasekhar SN explosions, Branch & Nomoto 1986; Woosley et al. 1986; Livne & Glasner 1990; Iben et al. 1997; Bildsten et al. 2007; Perets et al. 2010; Waldman et al. 2011; WD mergers Pakmor et al. 2013; NS-WD mergers; e.g. Margalit & Metzger 2016; and WD collisions; e.g. Papish & Perets 2016). Further studies of these channels using our newly developed detailed hybrid WD models will be further explored in forthcoming publications.

ACKNOWLEDGEMENTS

We thank Bill Wolf, Rob Farmer, Ylva Gotberg, and Erez Michaely for stimulating discussions. We acknowledge support from the Israel Science Foundation I-CORE grant 1829/12. ST acknowledges support from the Netherlands Research Council NWO (grant VENI [#639.041.645]).

REFERENCES

- Abt H. A., 1983, *ARA&A*, 21, 343
 Althaus L. G., Córscico A. H., Gauschy A., Han Z., Serenelli A. M., Panei J. A., 2004, *MNRAS*, 347, 125
 Bildsten L., Shen K. J., Weinberg N. N., Nelemans G., 2007, *ApJ*, 662, L95
 Branch D., Nomoto K., 1986, *A&A*, 164, L13
 Darwin G., 1879, *Phil. Trans. R. Soc.*, 170, 447
 De Rosa R. J. et al., 2014, *MNRAS*, 437, 1216
 Denissenkov P. A., Herwig F., Truran J. W., Paxton B., 2013, *ApJ*, 772, 37
 Duchêne G., Kraus A., 2013, *ARA&A*, 51, 269
 Farmer R., Fields C. E., Petermann I., Dessart L., Cantiello M., Paxton B., Timmes F. X., 2016, *ApJS*, 227, 22
 Han Z., Podsiadlowski P., Maxted P. F. L., Marsh T. R., Ivanova N., 2002, *MNRAS*, 336, 449
 Heggie D. C., 1975, *MNRAS*, 173, 729
 Hurley J. R., Pols O. R., Tout C. A., 2000, *MNRAS*, 315, 543
 Iben I., Jr, 1967, *ApJ*, 147, 650
 Iben I., Jr, Tutukov A. V., 1985, *ApJS*, 58, 661
 Iben I., Jr, Nomoto K., Tornambe A., Tutukov A. V., 1987, *ApJ*, 317, 717
 Iben I. J., Tutukov A. V., Yungelson L. R., 1997, *ApJ*, 475, 291
 Istrate A. G., Marchant P., Tauris T. M., Langer N., Stancliffe R. J., Grassitelli L., 2016, *A&A*, 595, A35
 Ivanova N. et al., 2013, *A&AR*, 21, 59
 Kippenhahn R., Weigert A., 1990, *Stellar Structure and Evolution*
 Kroupa P., Tout C. A., Gilmore G., 1993, *MNRAS*, 262, 545
 Livio M., Soker N., 1988, *ApJ*, 329, 764
 Livne E., Glasner A. S., 1990, *ApJ*, 361, 244
 Margalit B., Metzger B. D., 2016, *MNRAS*, 461, 1154
 Marsh T. R., Dhillon V. S., Duck S. R., 1995, *MNRAS*, 275, 828
 Mocák M., Campbell S. W., Müller E., Kifonidis K., 2010, *A&A*, 520, A114
 Nelemans G., 2010, *Ap&SS*, 329, 25
 Nelemans G., Verbunt F., Yungelson L. R., Portegies Zwart S. F., 2000, *A&A*, 360, 1011
 Nelemans G., Yungelson L. R., Portegies Zwart S. F., Verbunt F., 2001a, *A&A*, 365, 491
 Nelemans G., Portegies Zwart S. F., Verbunt F., Yungelson L. R., 2001b, *A&A*, 368, 939
 Paczyński B., 1971, *AcA*, 21, 417
 Paczynski B., 1976, in Eggleton P., Mitton S., Whelan J., eds, *IAU Symp. 73, Structure and Evolution of Close Binary Systems*. Kluwer, Dordrecht, 75
 Pakmor R., Kromer M., Taubenberger S., Springel V., 2013, *ApJ*, 770, L8
 Panei J. A., Althaus L. G., Benvenuto O. G., 2000, *A&A*, 353, 970
 Panei J. A., Althaus L. G., Chen X., Han Z., 2007, *MNRAS*, 382, 779
 Papish O., Perets H. B., 2016, *ApJ*, 822, 19
 Paxton B., Bildsten L., Dotter A., Herwig F., Lesaffre P., Timmes F., 2011, *ApJS*, 192, 3
 Paxton B. et al., 2015, *ApJS*, 220, 15
 Perets H. B. et al., 2010, *Nature*, 465, 322
 Portegies Zwart S. F., Verbunt F., 1996, *A&A*, 309, 179
 Prada Moroni P. G., Straniero O., 2009, *A&A*, 507, 1575
 Raghavan D. et al., 2010, *ApJS*, 190, 1
 Rebassa-Mansergas A., Nebot Gómez-Morán A., Schreiber M. R., Girven J., Gänsicke B. T., 2011, *MNRAS*, 413, 1121
 Toonen S., Nelemans G., 2013, *A&A*, 557, A87
 Toonen S., Nelemans G., Portegies Zwart S., 2012, *A&A*, 546, A70
 Toonen S., Claeys J. S. W., Mennekens N., Ruiter A. J., 2014, *A&A*, 562, A14
 Toonen S., Hollands M., Gänsicke B. T., Boekholt T., 2017, *A&A*, 602, A16
 Tutukov A., Yungelson L., 1979, in Conti P. S., De Loore C. W. H., eds, *IAU Symp. 83, Mass Loss and Evolution of O-Type Stars*. Kluwer, Dordrecht, p. 401
 Tutukov A. V., Yungelson L. R., 1992, *Sov. Astron.*, 36, 266
 Waldman R., Sauer D., Livne E., Perets H., Glasner A., Mazzali P., Truran J. W., Gal-Yam A., 2011, *ApJ*, 738, 21
 Webbink R. F., 1984, *ApJ*, 277, 355
 Winget D. E., Kepler S. O., 2008, *ARA&A*, 46, 157
 Woosley S. E., Taam R. E., Weaver T. A., 1986, *ApJ*, 301, 601
 Yungelson L. R., Kuranov A. G., 2017, *MNRAS*, 464, 1607
 Zhang X., Hall P. D., Jeffery C. S., Bi S., 2018, *MNRAS*, 474, 427

This paper has been typeset from a $\text{\TeX}/\text{\LaTeX}$ file prepared by the author.